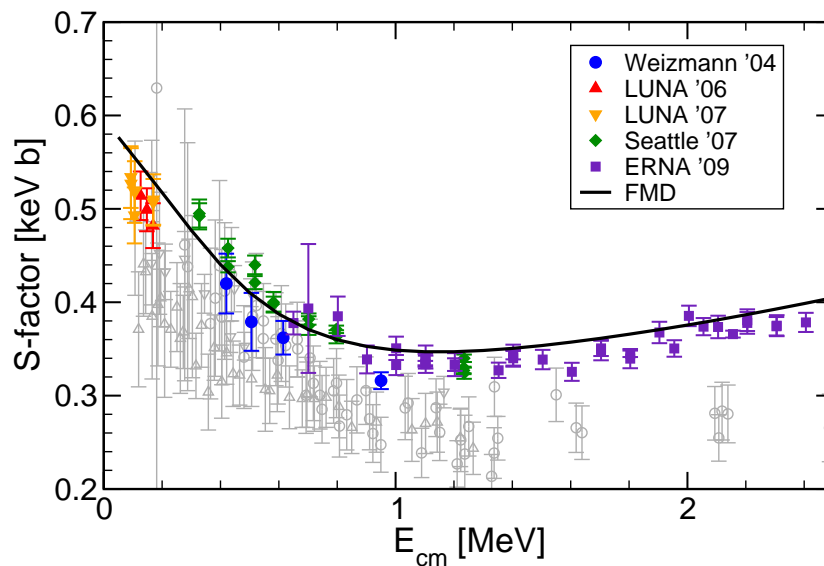


Microscopic calculation of the ${}^3\text{He}(\alpha, \gamma){}^7\text{Be}$ reaction rate



Thomas Neff
DREB 2012
Direct Reactions with
Exotic Beams
Pisa, Italy
Mar 26-30, 2012

Overview



Introduction

Effective interaction and many-body approach

- Unitary Correlation Operator Method
- Fermionic Molecular Dynamics

Results

- Bound and scattering states
- Astrophysical S -factor

Discussion

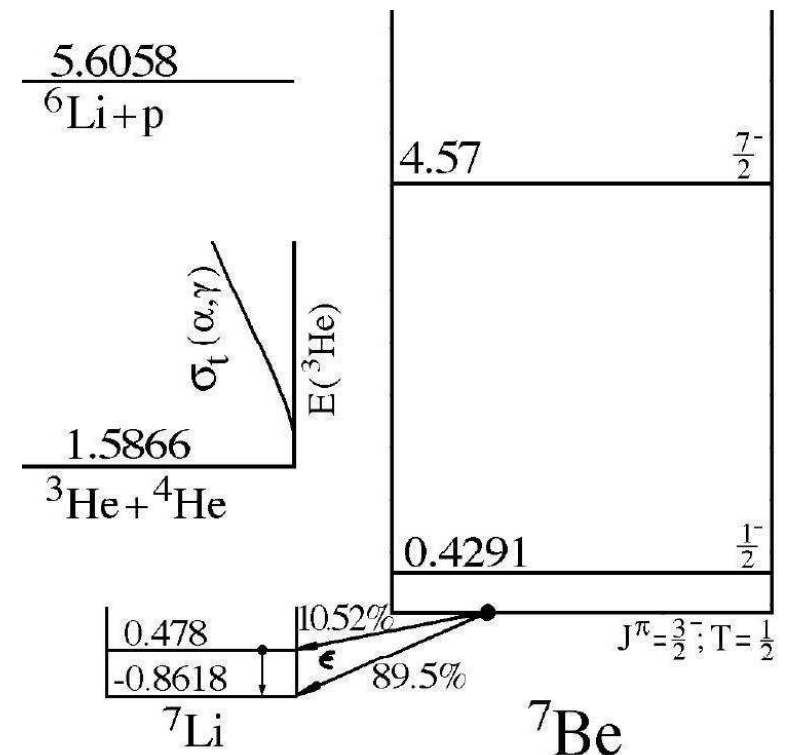
- Dipole matrix elements
- ${}^3\text{He}(\alpha, \gamma){}^7\text{Be}$ vs. ${}^3\text{H}(\alpha, \gamma){}^7\text{Li}$

Motivation

- ${}^3\text{He}(\alpha, \gamma){}^7\text{Be}$ one of the key reactions in the solar pp-chains
- in competition with the ${}^3\text{He}({}^3\text{He}, 2p){}^4\text{He}$ reaction it determines production of ${}^7\text{Be}$ and ${}^8\text{B}$ neutrinos

What is needed ?

- ${}^7\text{Be}$ bound state energies
- ${}^7\text{Be}$ bound state wave functions, ANC
- ${}^3\text{He}$ - ${}^4\text{He}$ scattering states
- dipole matrix elements between bound and scattering states



Theoretical Approaches

Potential models (Kim *et al.* 1982, Mohr 2009, ...)

- ${}^4\text{He}$ and ${}^3\text{He}$ are considered as point-like particles
- interacting via an effective nucleus-nucleus potential fitted to bound state properties and phase shifts
- ANCs calculated from *ab initio* wave functions (Nollett 2001, Navratil *et al.* 2007)

Microscopic Cluster Model (Tang *et al.* 1981, Langanke 1986, Kajino 1986 ...)

- antisymmetrized wave function built with ${}^4\text{He}$ and ${}^3\text{He}$ clusters
- some attempts to include polarization effects by adding other channels like ${}^6\text{Li}$ plus proton
- interacting via an effective nucleon-nucleon potential, adjusted to describe bound state properties and phase shifts

Our Aim

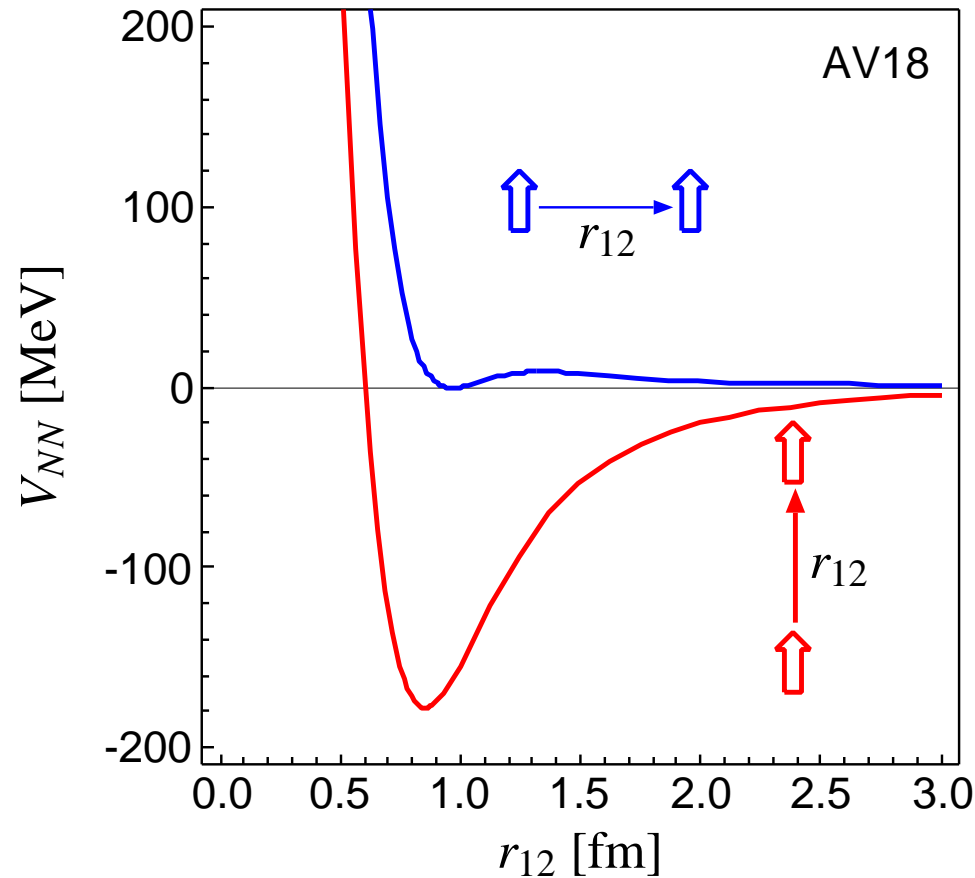
- fully microscopic wave functions with cluster configurations at large distances and additional polarized *A*-body configurations in the interaction region
- using a realistic effective interaction

Effective Interaction

Nuclear Force

Argonne V18 (T=0)

spins aligned parallel or perpendicular to the relative distance vector



- strong repulsive core: nucleons can not get closer than ≈ 0.5 fm

➤ **central correlations**

- strong dependence on the orientation of the spins due to the tensor force

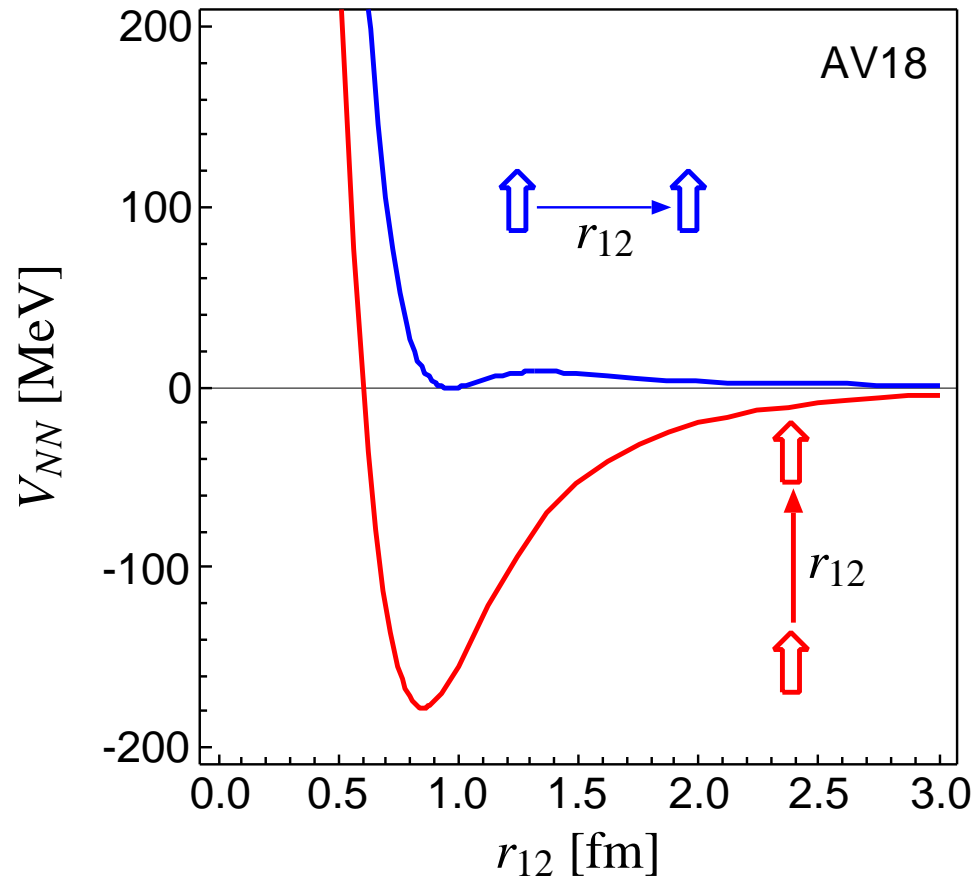
➤ **tensor correlations**

Effective Interaction

Nuclear Force

Argonne V18 (T=0)

spins aligned parallel or perpendicular to the relative distance vector



- strong repulsive core: nucleons can not get closer than ≈ 0.5 fm

➤ **central correlations**

- strong dependence on the orientation of the spins due to the tensor force

➤ **tensor correlations**

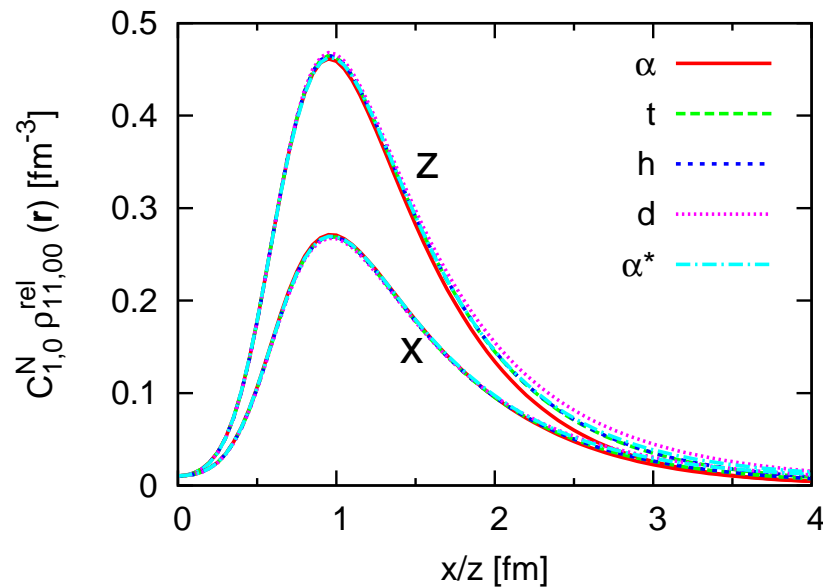
the nuclear force will induce **strong short-range correlations** in the nuclear wave function

Effective Interaction

Universality of short-range correlations

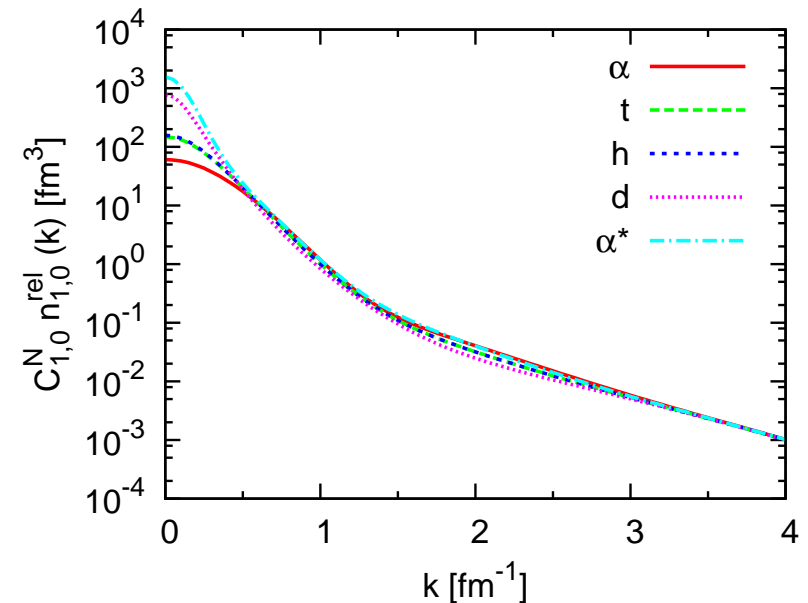
coordinate space

$$S = 1, M_S = 1, T = 0$$



momentum space

$$S = 1, T = 0$$



- normalize two-body density in coordinate space at $r=1.0$ fm
- normalized two-body densities in coordinate space are identical at short distances for all nuclei
- use the **same** normalization factor in momentum space – high momentum tails agree for all nuclei

Effective Interaction

Unitary Correlation Operator Method

Correlation Operator

- induce short-range (two-body) central and tensor correlations into the many-body state

$$\underline{\mathcal{C}} = \underline{\mathcal{C}}_{\Omega} \underline{\mathcal{C}}_r = \exp\left[-i \sum_{i < j} \underline{g}_{\Omega, ij}\right] \exp\left[-i \sum_{i < j} \underline{g}_{r, ij}\right] \quad , \quad \underline{\mathcal{C}}^{\dagger} \underline{\mathcal{C}} = \underline{1}$$

- correlation operator should conserve the symmetries of the Hamiltonian and should be of finite-range, correlated interaction **phase shift equivalent** to bare interaction by construction

Correlated Operators

- correlated operators will have contributions in higher cluster orders

$$\underline{\mathcal{C}}^{\dagger} \underline{O} \underline{\mathcal{C}} = \hat{\underline{O}}^{[1]} + \hat{\underline{O}}^{[2]} + \hat{\underline{O}}^{[3]} + \dots$$

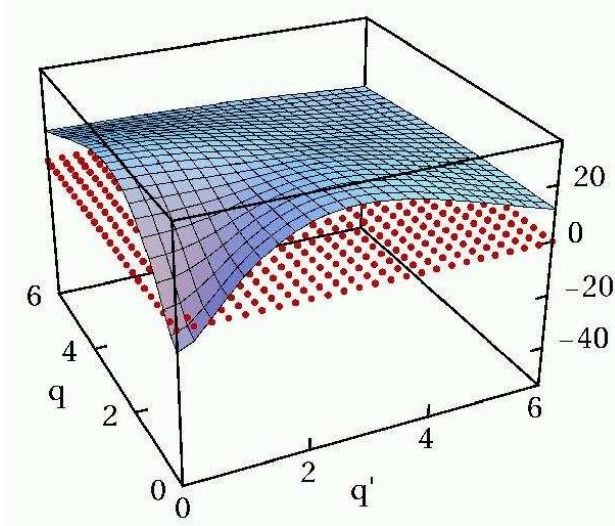
- two-body approximation: correlation range should be small compared to mean particle distance

Correlated Interaction

$$\underline{\mathcal{C}}^{\dagger} (\underline{T} + \underline{V}) \underline{\mathcal{C}} = \underline{T} + \underline{V}_{\text{UCOM}} + \underline{V}_{\text{UCOM}}^{[3]} + \dots$$

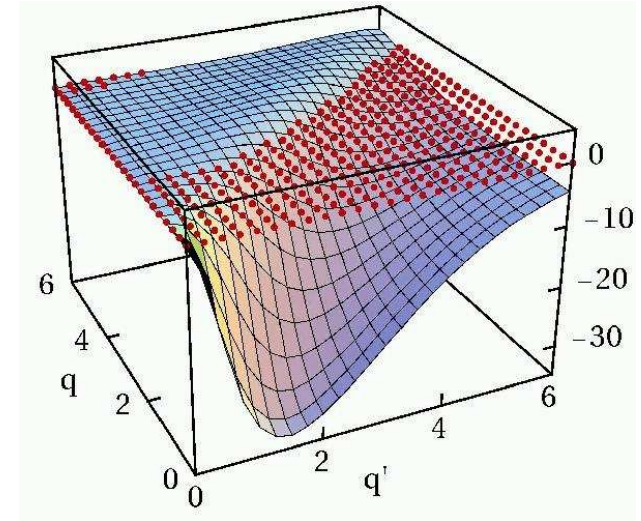
- Effective Interaction
- UCOM Interaction in Momentum Space $V(q, q')$

3S_1 bare



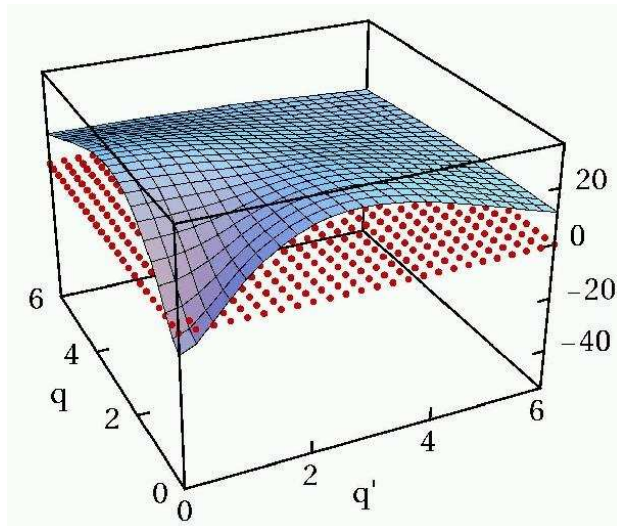
bare interaction has
strong
off-diagonal matrix
elements connecting
to high momenta

${}^3S_1 - {}^3D_1$ bare



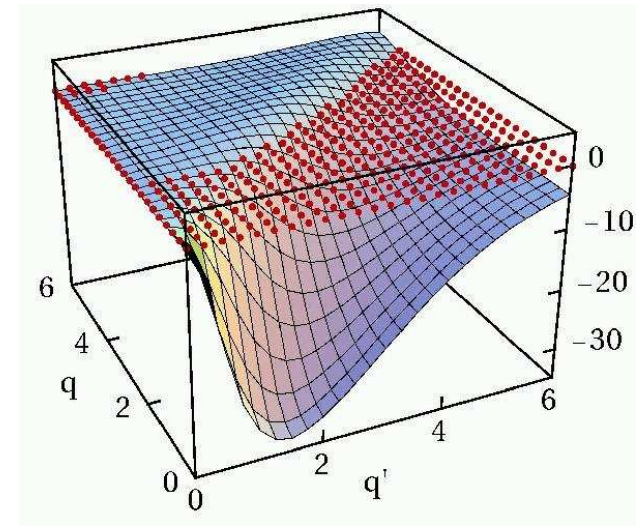
- Effective Interaction
- UCOM Interaction in Momentum Space $V(q, q')$

3S_1 bare



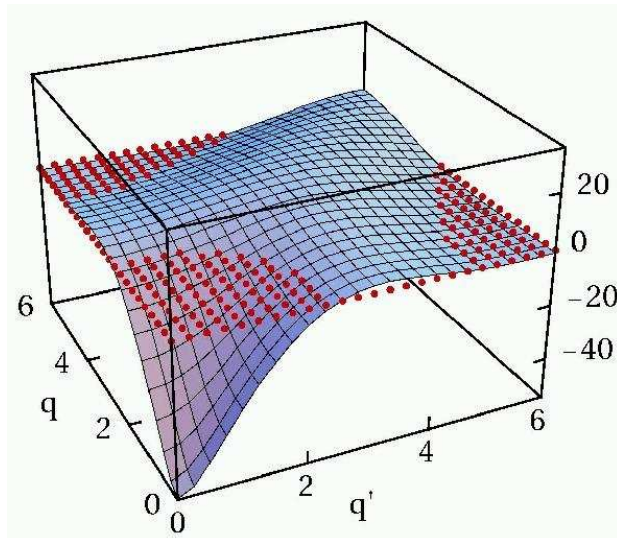
bare interaction has **strong off-diagonal** matrix elements connecting to high momenta

$^3S_1 - ^3D_1$ bare



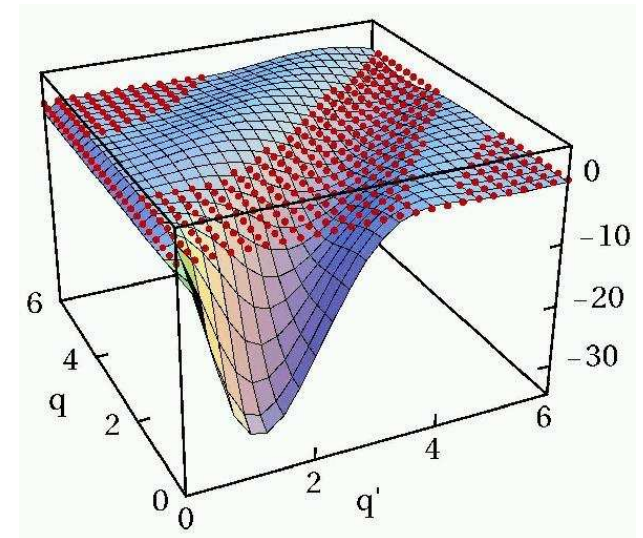
correlated interaction is **more attractive** at low momenta

3S_1 correlated



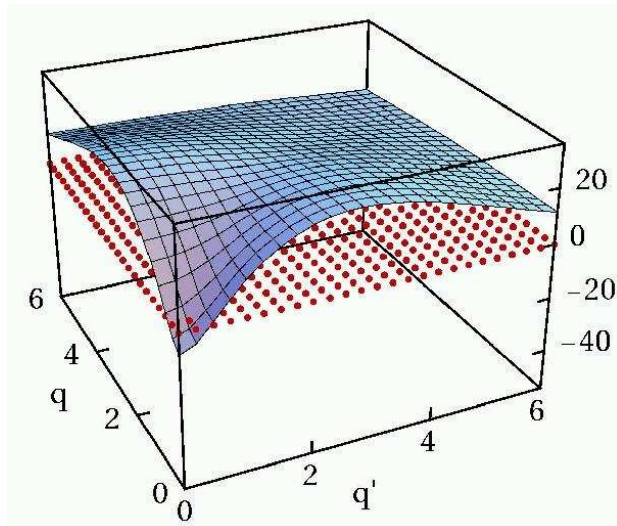
off-diagonal matrix elements connecting low- and high- momentum states are **strongly reduced**

$^3S_1 - ^3D_1$ correlated



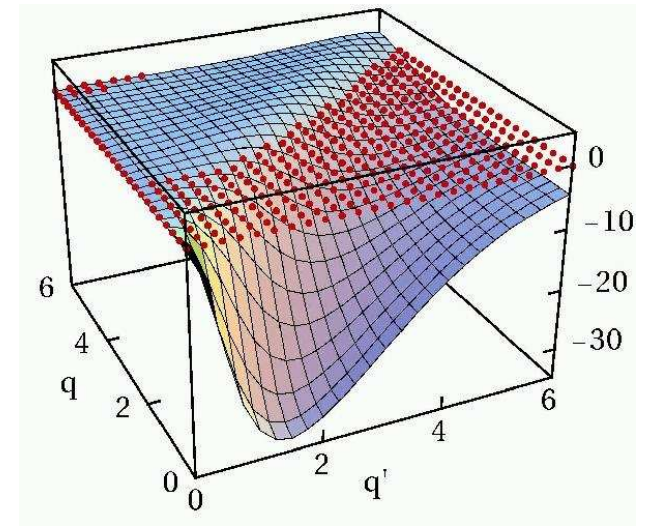
- Effective Interaction
- UCOM Interaction in Momentum Space $V(q, q')$

3S_1 bare



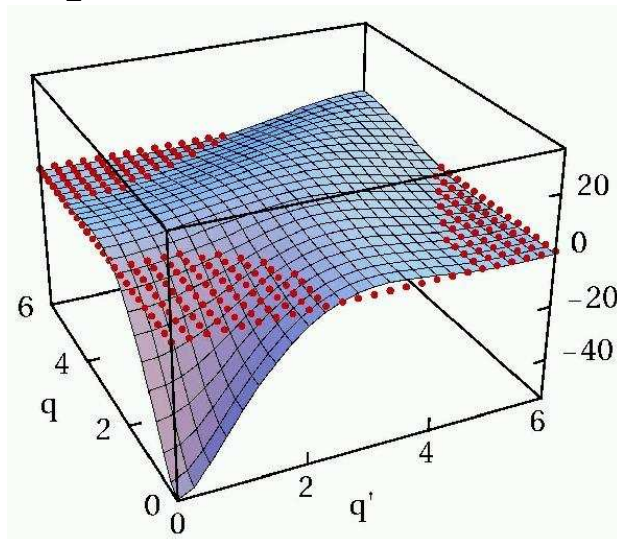
bare interaction has
strong off-diagonal matrix
elements connecting
to high momenta

$^3S_1 - ^3D_1$ bare



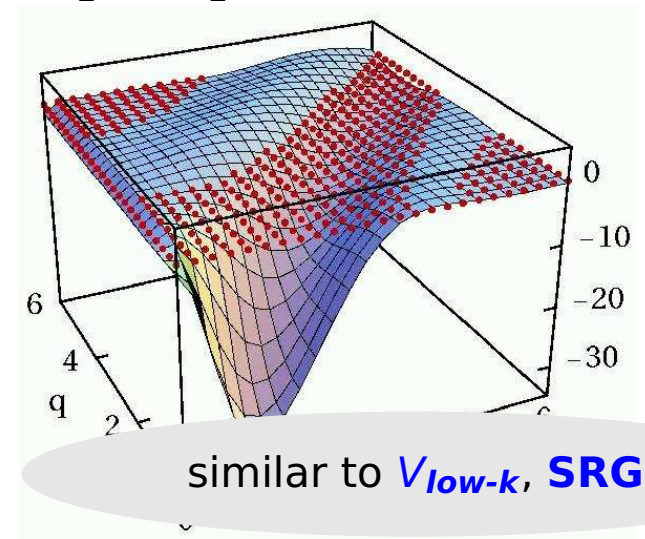
correlated interaction
is **more attractive**
at low momenta

3S_1 correlated



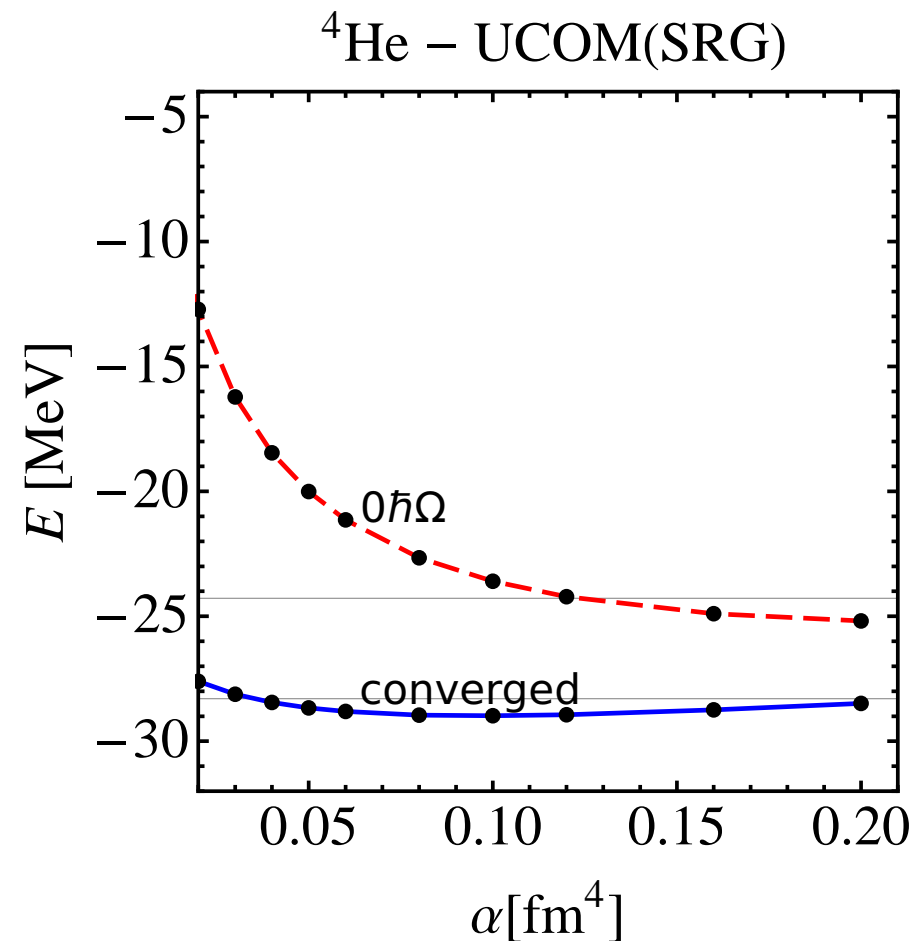
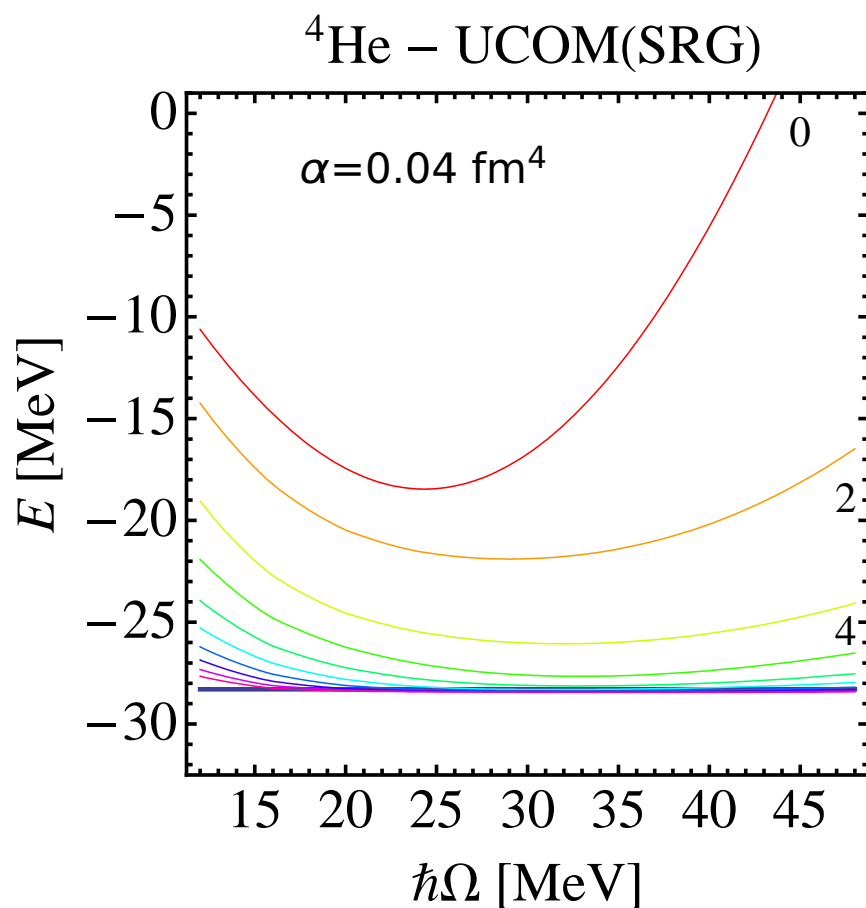
**off-diagonal
matrix elements**
connecting low- and
high- momentum
states are **strongly
reduced**

$^3S_1 - ^3D_1$ correlated



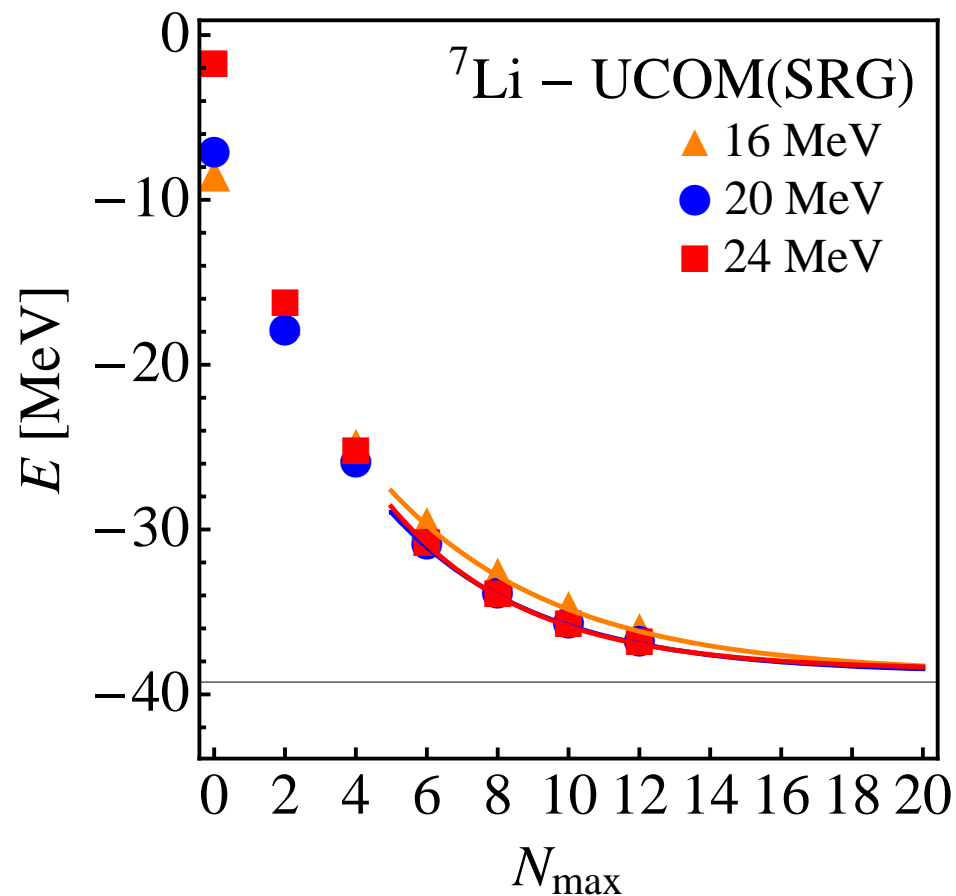
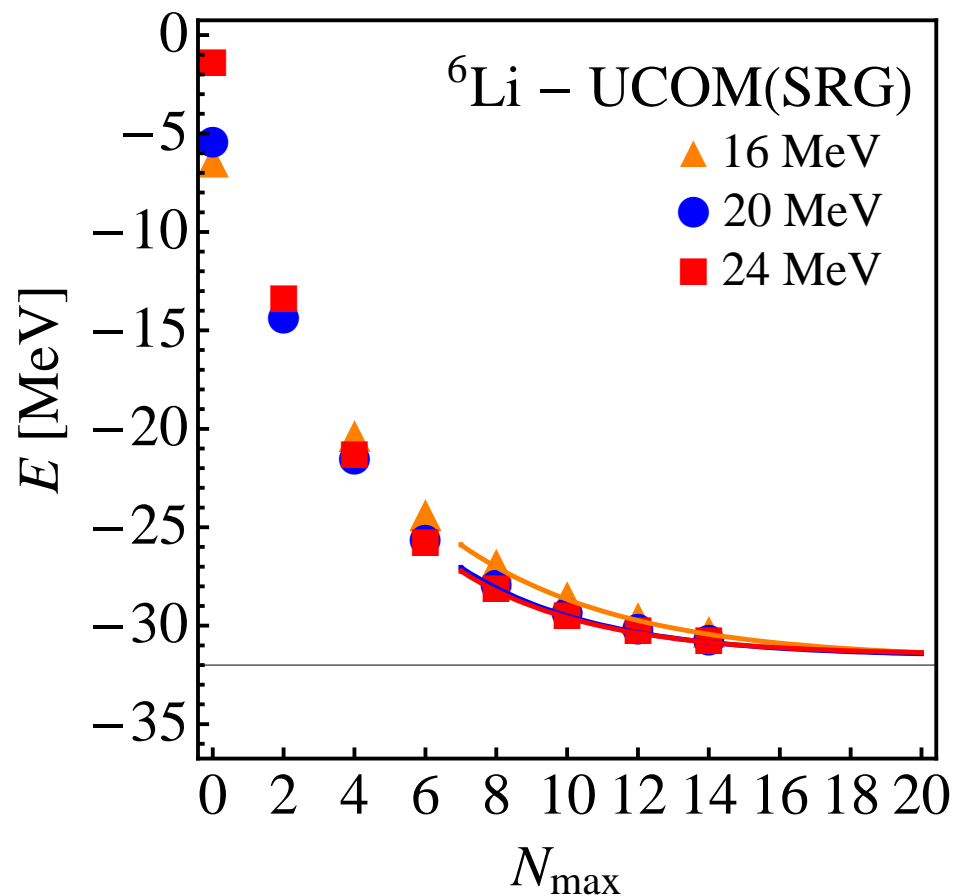
similar to V_{low-k} , **SRG**

- Effective Interaction
- No-Core Shell Model Calculations



- convergence much improved compared to bare interaction
- effective interaction – in two-body approximation – converges to different energy than bare interaction
- transformed interaction can be tuned to obtain simultaneously (almost) exact ${}^3\text{He}$ and ${}^4\text{He}$ binding energies

- Effective Interaction
- NCSM ${}^6\text{Li}/{}^7\text{Li}$ ground state energy



- effective interaction also works reasonably well for heavier nuclei

- Many-body Approach
- Fermionic Molecular Dynamics

Fermionic

Slater determinant

$$|Q\rangle = \mathcal{A}\left(|q_1\rangle \otimes \cdots \otimes |q_A\rangle\right)$$

- antisymmetrized A -body state

Feldmeier, Schnack, Rev. Mod. Phys. **72** (2000) 655

Neff, Feldmeier, Nucl. Phys. **A738** (2004) 357

Many-body Approach Fermionic Molecular Dynamics

Fermionic

Slater determinant

$$|Q\rangle = \mathcal{A}\left(|q_1\rangle \otimes \cdots \otimes |q_A\rangle\right)$$

- antisymmetrized A -body state

Molecular

single-particle states

$$\langle \mathbf{x} | q \rangle = \sum_i c_i \exp\left\{-\frac{(\mathbf{x} - \mathbf{b}_i)^2}{2a_i}\right\} \otimes |x_i^\uparrow, x_i^\downarrow\rangle \otimes |\xi\rangle$$

- Gaussian wave-packets in phase-space (complex parameter \mathbf{b}_i encodes mean position and mean momentum), spin is free, isospin is fixed
- width a_i is an independent variational parameter for each wave packet
- use one or two wave packets for each single particle state

Feldmeier, Schnack, Rev. Mod. Phys. **72** (2000) 655

Neff, Feldmeier, Nucl. Phys. **A738** (2004) 357

Many-body Approach Fermionic Molecular Dynamics

Fermionic

Slater determinant

$$|Q\rangle = \mathcal{A}\left(|q_1\rangle \otimes \cdots \otimes |q_A\rangle\right)$$

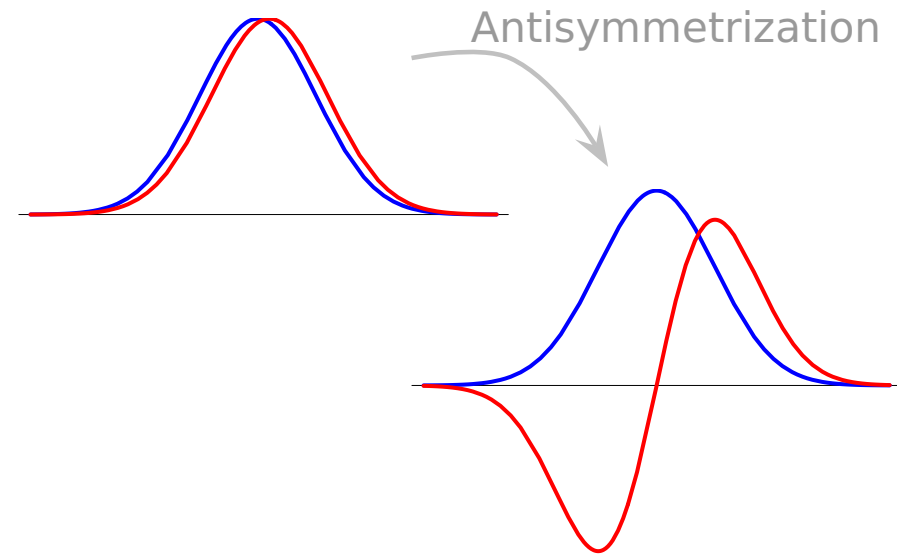
- antisymmetrized A-body state

Molecular

single-particle states

$$\langle \mathbf{x} | q \rangle = \sum_i c_i \exp\left\{-\frac{(\mathbf{x} - \mathbf{b}_i)^2}{2a_i}\right\} \otimes |\chi_i^\uparrow, \chi_i^\downarrow\rangle \otimes |\xi\rangle$$

- Gaussian wave-packets in phase-space (complex parameter \mathbf{b}_i encodes mean position and mean momentum), spin is free, isospin is fixed
- width a_i is an independent variational parameter for each wave packet
- use one or two wave packets for each single particle state



Many-body Approach Fermionic Molecular Dynamics

Fermionic

Slater determinant

$$|Q\rangle = \mathcal{A}\left(|q_1\rangle \otimes \cdots \otimes |q_A\rangle\right)$$

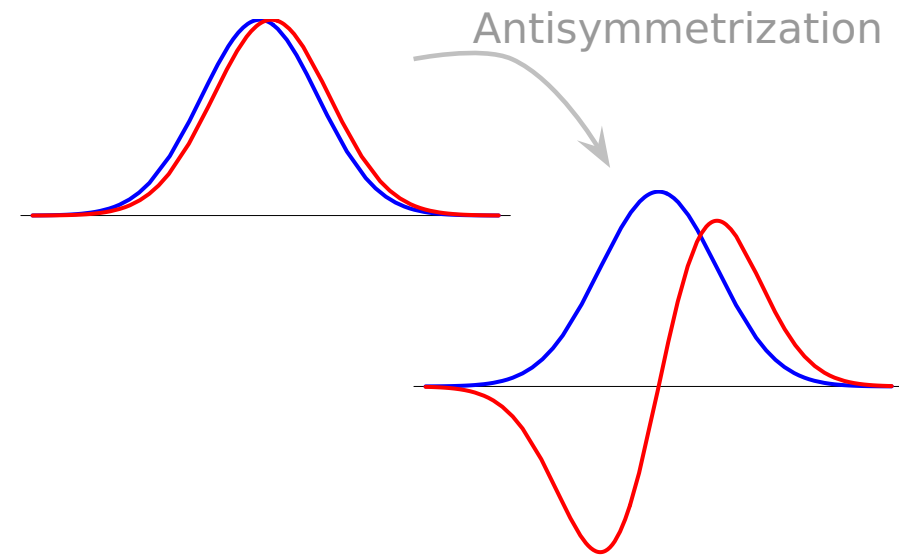
- antisymmetrized A-body state

Molecular

single-particle states

$$\langle \mathbf{x} | q \rangle = \sum_i c_i \exp\left\{-\frac{(\mathbf{x} - \mathbf{b}_i)^2}{2a_i}\right\} \otimes |\chi_i^\uparrow, \chi_i^\downarrow\rangle \otimes |\xi\rangle$$

- Gaussian wave-packets in phase-space (complex parameter \mathbf{b}_i encodes mean position and mean momentum), spin is free, isospin is fixed
- width a_i is an independent variational parameter for each wave packet
- use one or two wave packets for each single particle state



see also
**Antisymmetrized
Molecular Dynamics**
Horiuchi, Kanada-En'yo,
Kimura, ...

Feldmeier, Schnack, Rev. Mod. Phys. **72** (2000) 655

Neff, Feldmeier, Nucl. Phys. **A738** (2004) 357

• Many-body Approach • Restoration of Symmetries

Projection After Variation (PAV)

- mean-field may break symmetries of Hamiltonian
- restore inversion, translational and rotational symmetry by projection on parity, linear and angular momentum

$$\tilde{P}^{\pi} = \frac{1}{2}(1 + \pi \tilde{\Pi})$$

$$\tilde{P}_{MK}^J = \frac{2J+1}{8\pi^2} \int d^3\Omega D_{MK}^{J*}(\Omega) \tilde{R}(\Omega)$$

$$\tilde{P}^{\mathbf{P}} = \frac{1}{(2\pi)^3} \int d^3\mathbf{X} \exp\{-i(\tilde{\mathbf{P}} - \mathbf{P}) \cdot \mathbf{X}\}$$

Many-body Approach Restoration of Symmetries

Projection After Variation (PAV)

- mean-field may break symmetries of Hamiltonian
- restore inversion, translational and rotational symmetry by projection on parity, linear and angular momentum

$$\tilde{P}^{\pi} = \frac{1}{2}(1 + \pi \tilde{\Pi})$$

$$\tilde{P}_{MK}^J = \frac{2J+1}{8\pi^2} \int d^3\Omega D_{MK}^{J*}(\Omega) \tilde{R}(\Omega)$$

Variation After Projection (VAP)

- effect of projection can be large
- full **Variation after Angular Momentum and Parity Projection** (VAP) for light nuclei
- perform VAP in GCM sense by applying **constraints** on radius, dipole moment, quadrupole moment or octupole moment and minimizing the energy in the projected energy surface for heavier nuclei

$$\tilde{P}^{\mathbf{P}} = \frac{1}{(2\pi)^3} \int d^3\mathbf{X} \exp\{-i(\tilde{\mathbf{P}} - \mathbf{P}) \cdot \mathbf{X}\}$$

Many-body Approach Restoration of Symmetries

Projection After Variation (PAV)

- mean-field may break symmetries of Hamiltonian
- restore inversion, translational and rotational symmetry by projection on parity, linear and angular momentum

$$\tilde{P}^{\pi} = \frac{1}{2}(1 + \pi \tilde{\Pi})$$

$$\tilde{P}_{MK}^J = \frac{2J+1}{8\pi^2} \int d^3\Omega D_{MK}^{J*}(\Omega) \tilde{P}(\Omega)$$

Variation After Projection (VAP)

- effect of projection can be large
- full **Variation after Angular Momentum and Parity Projection** (VAP) for light nuclei
- perform VAP in GCM sense by applying **constraints** on radius, dipole moment, quadrupole moment or octupole moment and minimizing the energy in the projected energy surface for heavier nuclei

$$\tilde{P}^{\mathbf{P}} = \frac{1}{(2\pi)^3} \int d^3\mathbf{X} \exp\{-i(\tilde{\mathbf{P}} - \mathbf{P}) \cdot \mathbf{X}\}$$

Multiconfiguration Calculations

- diagonalize** Hamiltonian in a set of projected intrinsic states

$$\left\{ |Q^{(a)}\rangle, \quad a = 1, \dots, N \right\}$$

$$\sum_{K'b} \langle Q^{(a)} | H \tilde{P}_{KK'}^{J\pi} \tilde{P}^{\mathbf{P}=0} | Q^{(b)} \rangle \cdot c_{K'b}^{\alpha} = E^{J\pi\alpha} \sum_{K'b} \langle Q^{(a)} | \tilde{P}_{KK'}^{J\pi} \tilde{P}^{\mathbf{P}=0} | Q^{(b)} \rangle \cdot c_{K'b}^{\alpha}$$

Frozen configurations

- antisymmetrized wave function built with ${}^4\text{He}$ and ${}^3\text{He}$ FMD clusters up to channel radius $a=12$ fm

Polarized configurations

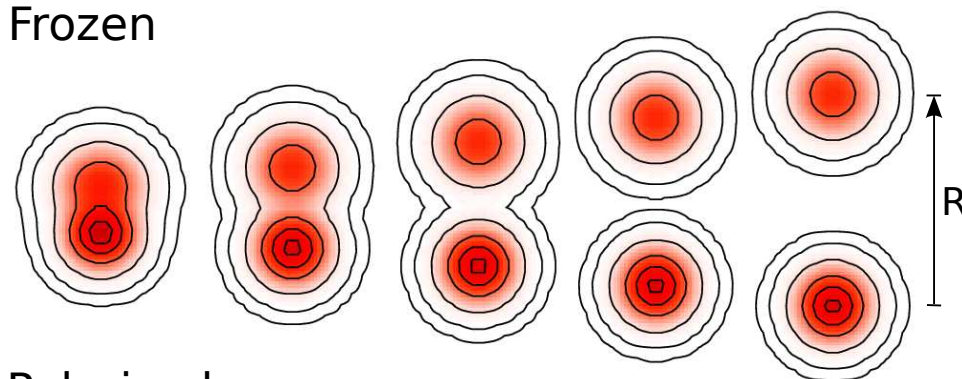
- FMD wave functions obtained by VAP on $1/2^-$, $3/2^-$, $5/2^-$, $7/2^-$ and $1/2^+$, $3/2^+$ and $5/2^+$ combined with radius constraint in the interaction region

Boundary conditions

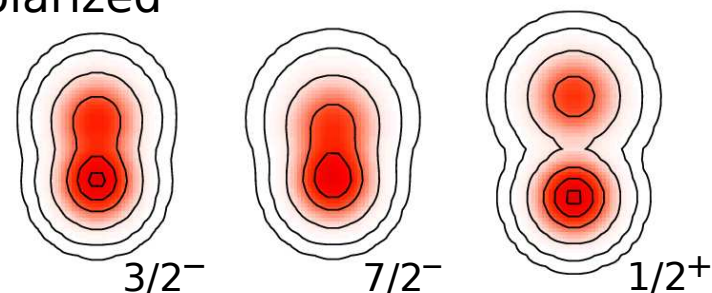
- Match relative motion of clusters at channel radius to Whittaker/Coulomb functions with the **microscopic R-matrix** method of the Brussels group

D. Baye, P.-H. Heenen, P. Descouvemont

Frozen



Polarized



$^3\text{He}(\alpha, \gamma)^7\text{Be}$ p -wave Bound and Scattering States

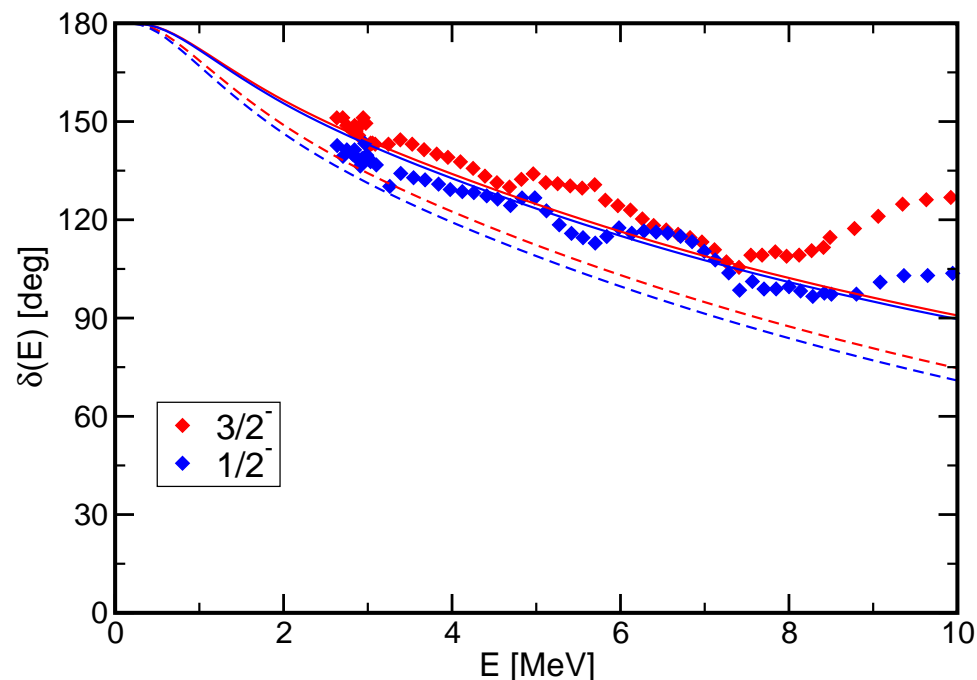
Bound states

		Experiment	FMD
^7Be	$E_{3/2-}$	-1.59 MeV	-1.49 MeV
	$E_{1/2-}$	-1.15 MeV	-1.31 MeV
	r_{ch}	2.647(17) fm	2.67 fm
	Q	–	-6.83 e fm ²
^7Li	$E_{3/2-}$	-2.467 MeV	-2.39 MeV
	$E_{1/2-}$	-1.989 MeV	-2.17 MeV
	r_{ch}	2.444(43) fm	2.46 fm
	Q	-4.00(3) e fm ²	-3.91 e fm ²

- centroid of bound state energies well described if polarized configurations included
- tail of wave functions tested by charge radii and quadrupole moments

Phase shift analysis:

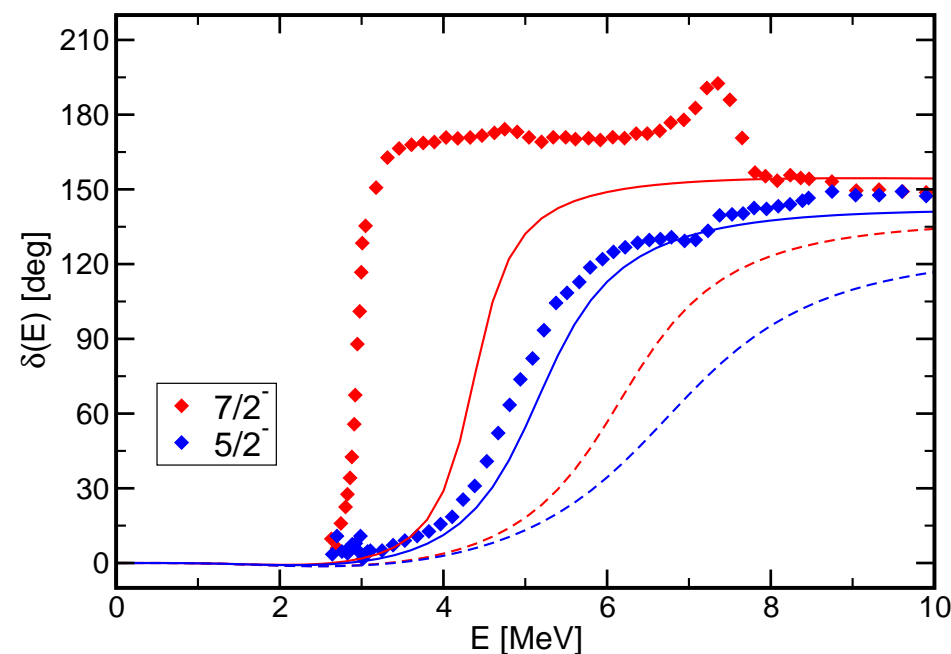
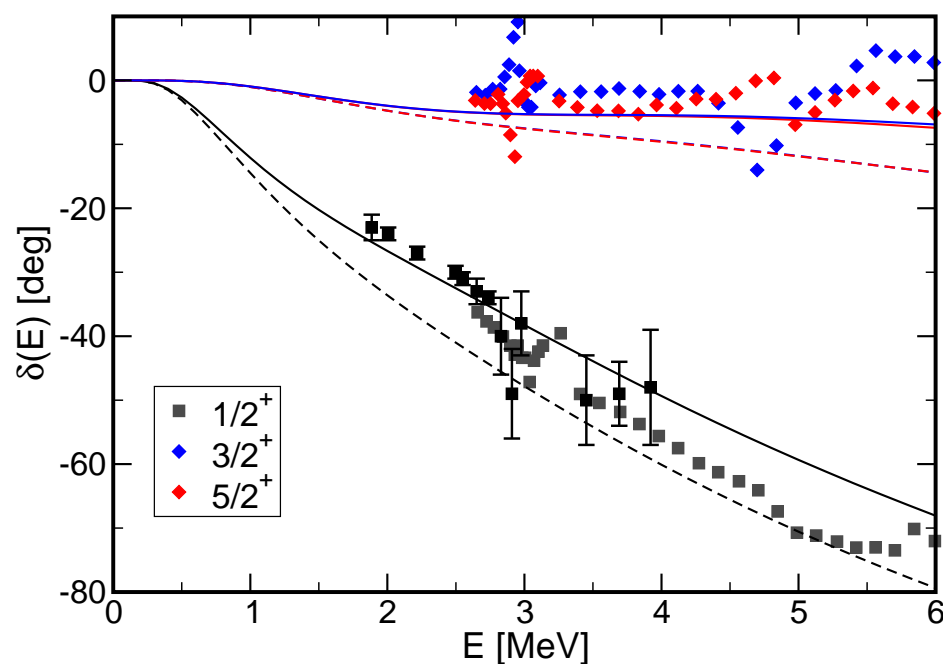
Spiger and Tombrello, PR **163**, 964 (1967)



dashed lines – frozen configurations only
solid lines – polarized configurations in interaction region included

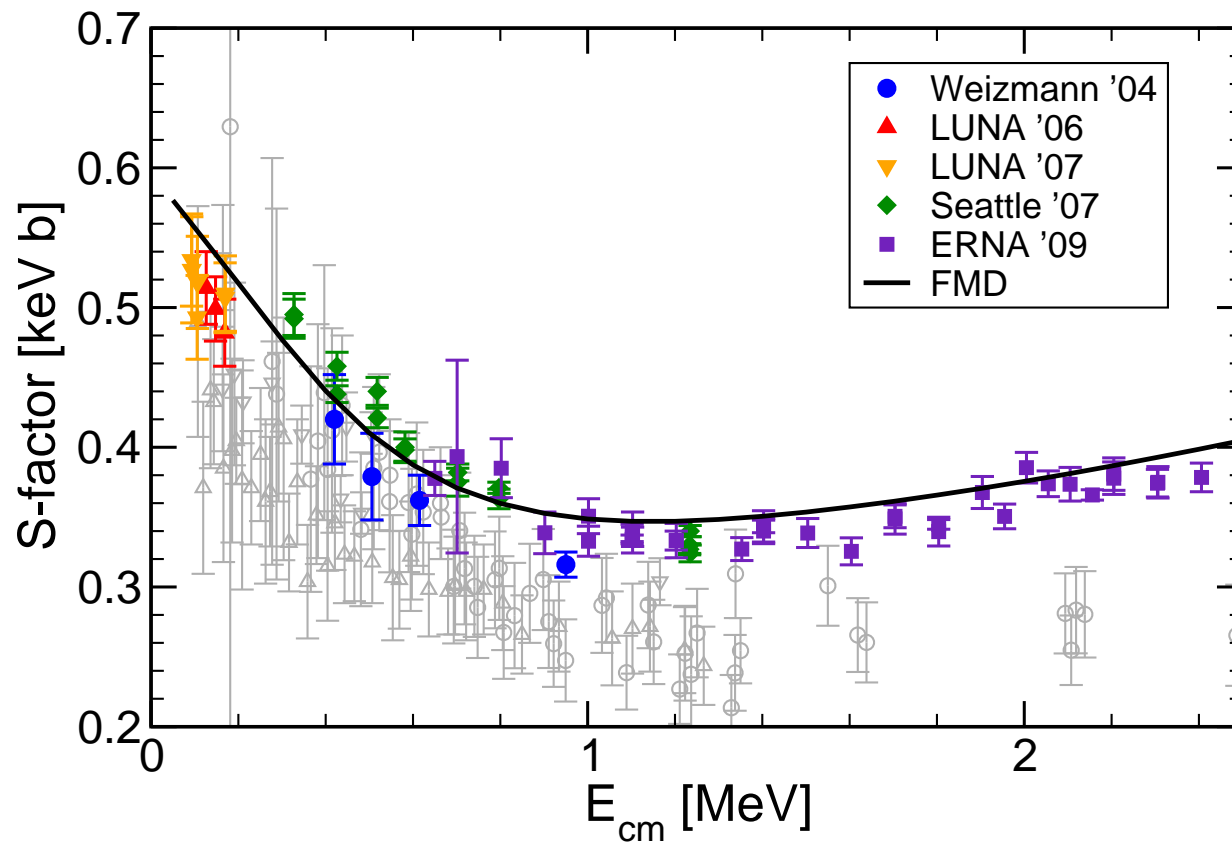
- Scattering phase shifts well described, polarization effects important

- ${}^3\text{He}(\alpha, \gamma){}^7\text{Be}$
- ***s*-, *d*- and *f*-wave Scattering States**



dashed lines – frozen configurations only – solid lines – FMD configurations in interaction region included

- polarization effects important
- *s*- and *d*-wave scattering phase shifts well described
- $7/2^-$ resonance too high, $5/2^-$ resonance roughly right, consistent with no-core shell model calculations

**S-factor:**

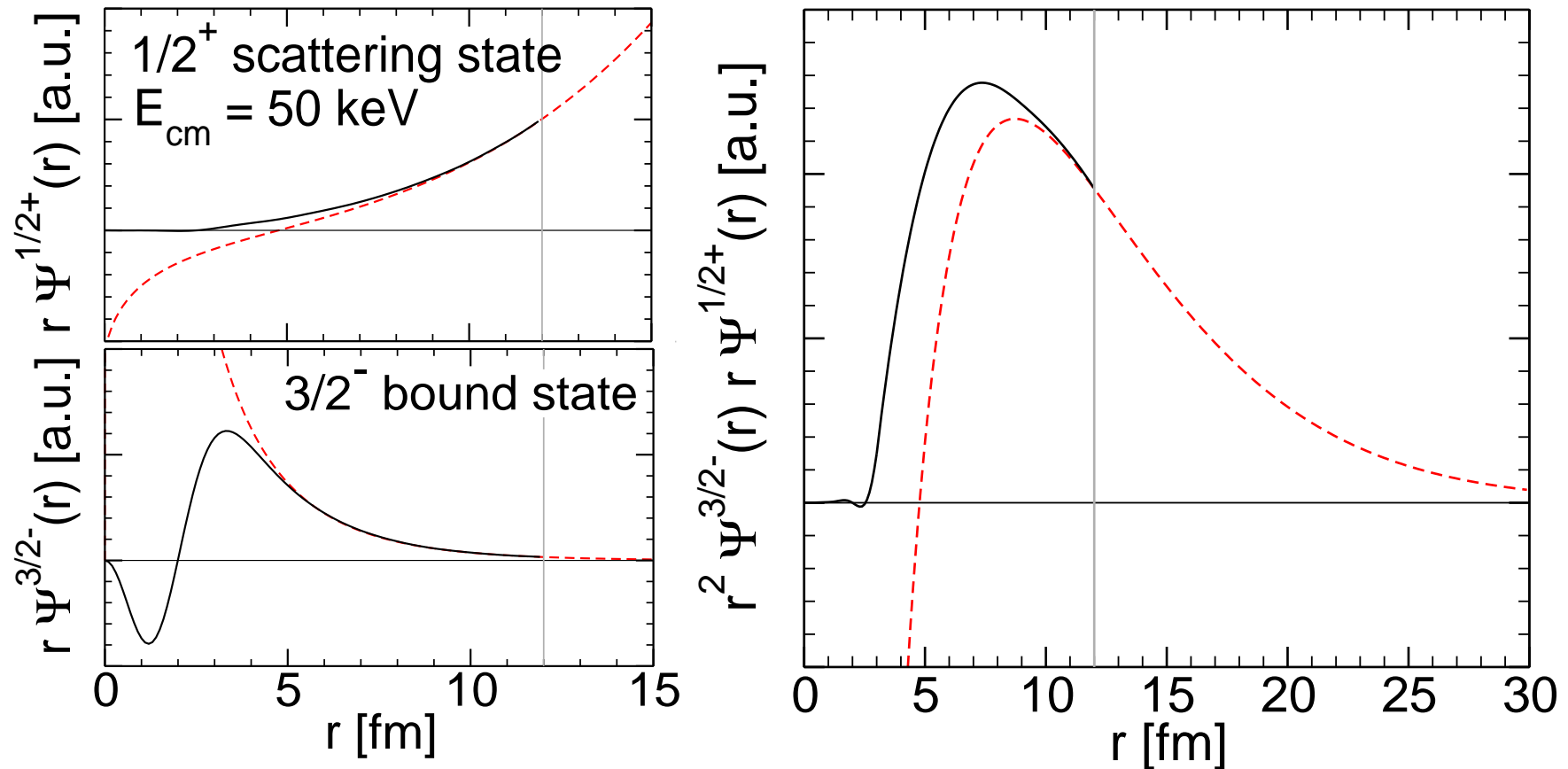
$$S(E) = \sigma(E)E \exp\{2\pi\eta\}$$

$$\eta = \frac{\mu Z_1 Z_2 e^2}{k}$$

Nara Singh *et al.*, PRL **93**, 262503 (2004)
Bemmerer *et al.*, PRL **97**, 122502 (2006)
Confortola *et al.*, PRC **75**, 065803 (2007)
Brown *et al.*, PRC **76**, 055801 (2007)
Di Leva *et al.*, PRL **102**, 232502 (2009)

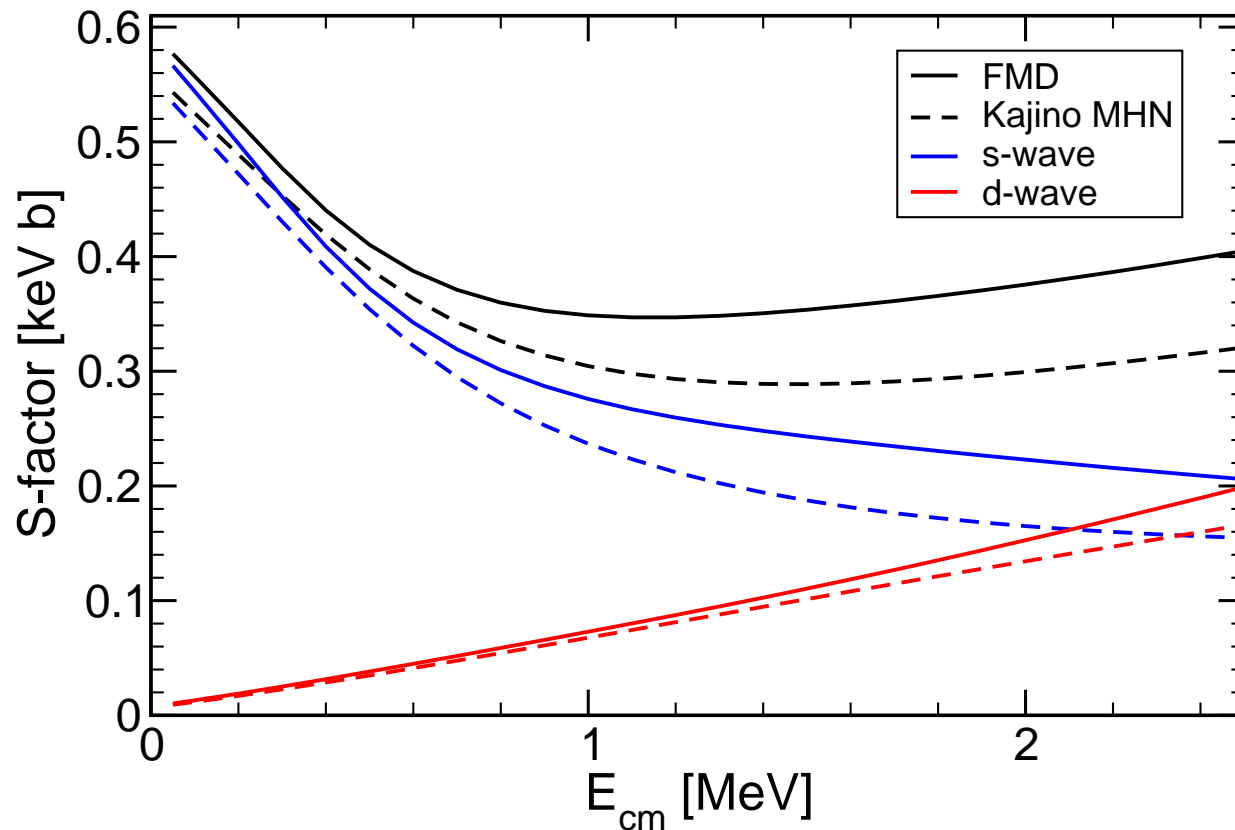
- dipole transitions from $1/2^+$, $3/2^+$, $5/2^+$ scattering states into $3/2^-$, $1/2^-$ bound states
- FMD is the only model that describes well the energy dependence and normalization of new high quality data
- fully microscopic calculation, bound and scattering states are described consistently

• Overlap Functions and Dipole Matrixelements



- Overlap functions from projection on RGM-cluster states
- Coulomb and Whittaker functions matched at channel radius $a=12$ fm
- Dipole matrix elements calculated from overlap functions reproduce full calculation within 2%
- cross section depends significantly on internal part of wave function, description as an “external” capture is too simplified

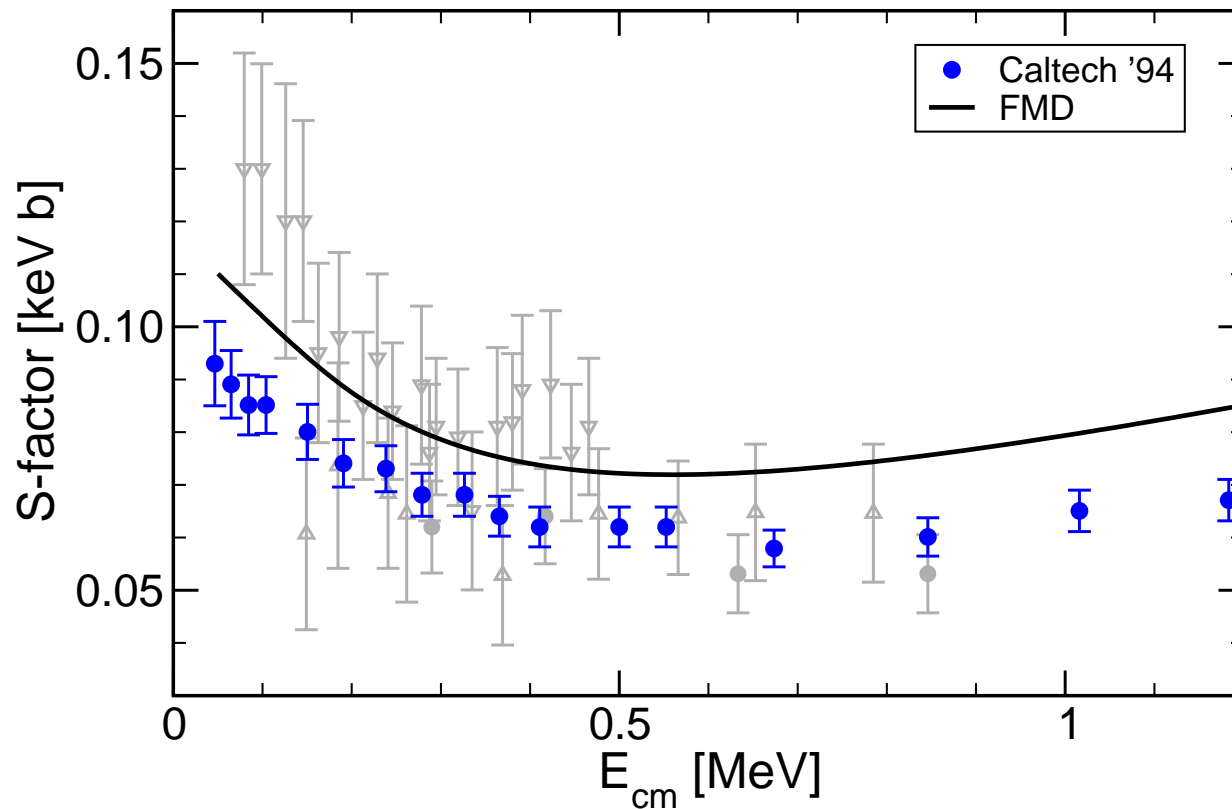
• **Energy dependence of the S-Factor**



- low-energy S -factor dominated by s -wave capture
- at 2.5 MeV equal contributions of s - and d -wave capture
- FMD results differ from Kajino results mainly with respect to s -wave capture
- related to short-range part of wave functions ?

$^3\text{H}(\alpha, \gamma)^7\text{Li}$

S-Factor



S-factor:

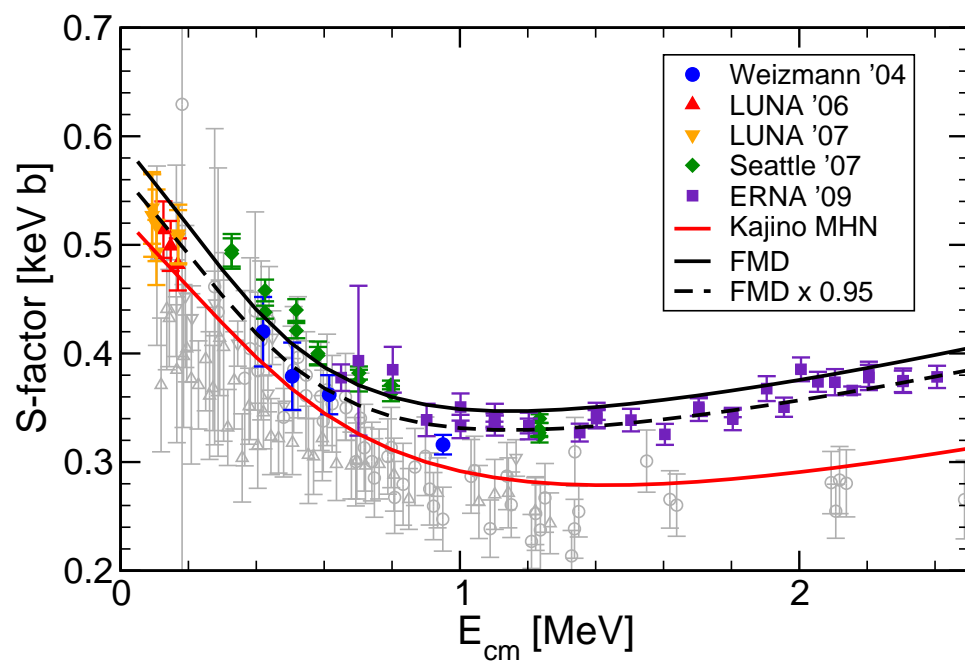
$$S(E) = \sigma(E)E \exp\{2\pi\eta\}$$
$$\eta = \frac{\mu Z_1 Z_2 e^2}{k}$$

Brune *et al.*, PRC **50**, 2205 (1994)

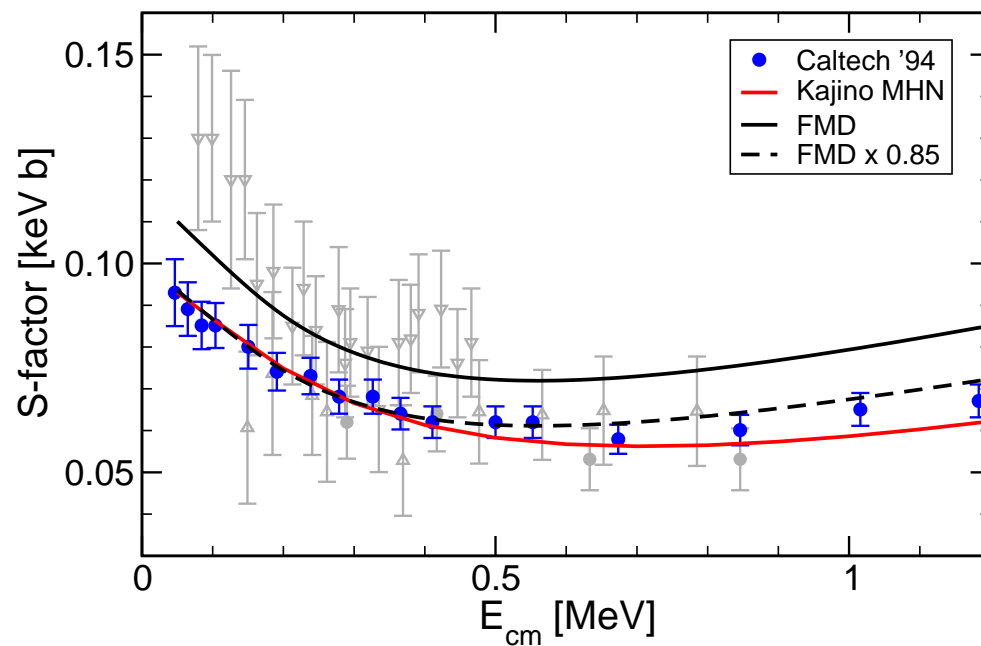
- isospin mirror reaction of $^3\text{He}(\alpha, \gamma)^7\text{Be}$
- ^7Li bound state properties and phase shifts well described
- ➔ FMD calculation describes energy dependence of Brune *et al.* data but cross section is larger by about 15%

$^3\text{He}(\alpha, \gamma)^7\text{Be}$ and $^3\text{H}(\alpha, \gamma)^7\text{Li}$ **S-Factors consistent ?**

$^3\text{He}(\alpha, \gamma)^7\text{Be}$



$^3\text{H}(\alpha, \gamma)^7\text{Li}$



- FMD calculation agrees with normalization and energy dependence of $^3\text{He}(\alpha, \gamma)^7\text{Be}$ data
- FMD calculation agrees with energy dependence but not normalization of $^3\text{H}(\alpha, \gamma)^7\text{Li}$ data
- similar inconsistency observed in other models

Summary

Effective interaction and many-body approach

- explicit inclusion of short-range central and tensor in the UCOM approach provides realistic low-momentum interaction
- FMD basis allows to describe frozen cluster configurations and polarized configurations in the interaction region

$^3\text{He}(\alpha, \gamma)^7\text{Be}$ Radiative Capture

- Bound states and scattering states wave functions
- S-factor: energy dependence and normalization agrees with data
- Overlap functions, dipole matrix elements
- $^3\text{He}(\alpha, \gamma)^7\text{Be}$ and $^3\text{H}(\alpha, \gamma)^7\text{Li}$ data inconsistent ?

PRL **106**, 042502 (2011)

PHYSICAL REVIEW LETTERS

week ending
28 JANUARY 2011

Microscopic Calculation of the $^3\text{He}(\alpha, \gamma)^7\text{Be}$ and $^3\text{H}(\alpha, \gamma)^7\text{Li}$ Capture Cross Sections Using Realistic Interactions

Thomas Neff*

GSI Helmholtzzentrum für Schwerionenforschung GmbH, Planckstraße 1, 64291 Darmstadt, Germany

(Received 12 November 2010; published 25 January 2011)